EFFECT OF BROMINE AND IODINE ON METHANOL AND METHANE FLAMES

C. Luo, B. Z. Dlugogorski and E. M. Kennedy*

Process Safety and Environment Protection Research Group
Priority Energy Research Centre, School of Engineering
The University of Newcastle, Callaghan, NSW 2308, AUSTRALIA
Phone: +61 2 4921 6176, Fax: +61 2 4921 6920
Email: Eric.Kennedy@newcastle.edu.au

ABSTRACT

A comprehensive kinetic mechanism, which combines the GRI (Gas Research Institute), hydrofluorocarbon (HFC) and modified $CF_3I/CBrF_3$ inhibition mechanisms is developed and used to study the flame structure, and disclose the key reaction pathways (based on bromine/iodine atom fluxes), influencing methane and methanol fuelled flames. The mechanism is tested against burning velocity and flame structures data obtained from the open literature.

The key reactions responsible for the flame suppression are established based, on their influence on the major inhibition cycles. In addition, the reaction pathways influencing fuel oxidation, and reactions of the agents based on bromine or iodine atom flux, were also assessed. Specifically, the reactions responsible for the difference in effectiveness of Br_2 and HBr over I_2 and HI in the methane-air and methanol-air premixed flames are identified.

Keywords: Heat release rate, flame promotion, burning velocity, flame inhibition mechanism, inhibition cycle.

1. INTRODUCTION

Moore et al. [1] reported that the concentration of CF_3I and $CBrF_3$ required to extinguish a methanol-fuelled flame are 3.8% and 5.9% by volume respectively. These data were obtained experimentally, from cup burner measurements, and suggests that for methanol flames, CF_3I is a more efficient agent than $CBrF_3$. In addition, the numerical analysis undertaken by Noto et al. [2, 3] predicts a substantially higher inhibition index for CF_3I than for $CBrF_3$ for CH_3OH flames, and these authors noted that the reaction of a bromine radical with the fuel (CH_3OH + Br) contributes significantly to regeneration of the flame inhibitor HBr. Luo et al. [4] employed heat release analysis and reaction pathway analysis to develop an explanation for the apparent higher suppressing efficiency of CF_3I over $CBrF_3$ for methanol flames.

In this paper, Luo et al. [4]'s assessment is developed further, and the flame extinguishing characteristics of I_2 over Br_2 and HI over HBr for methanol-air flames is studied. Sensitivity analysis for burning velocity and radical H is presented in order to identify the key reactions which are most sensitive to a change of the burning velocity and hydrogen atom radical concentration. In addition, reaction pathway analysis, based on the bromine/iodine atom flux, will be used to identify the reactions responsible for the effect of fuel type (methane and methanol) and develop an explanation for the difference in the effectiveness of I_2 over Br_2 and HI over HBr.

2. CHEMICAL KINETICS

The GRI-MECH 3.0 mechanism of Smith et al. [5] was adopted for C_4-hydrocarbon oxidation kinetics. Its thermodynamic database was used for both kinetic and

thermodynamic calculations. Reactions containing nitrogen species were removed from the mechanism. The National Institute of Standards and Technology (NIST) hydrofluorocarbon (HFC) mechanism by Burgess et al. [6], with its database provided thermochemical constants characterising hydrofluorocarbon oxidation chemistry. Adopting this HFC mechanism, some of the reaction coefficients were updated according to research undertaken by L'Esperance et al. [7] and Linteris and Gmurczyk [8]. The final comprehensive kinetic mechanism comprised 100 species and 880 reverse reaction steps for mechanisms 1, as listed in Table 1, and 101 species and 881 reverse reactions steps for mechanism 2.

Table 1 Summary of the detailed kinetic mechanisms used in the present study

Mechanism	Sub-mechanisms	No. of species	No. of reactions
1	GRI - Mech 3.0 + NIST HFC + Modified NIST $CBrF_3$	100	880
2	GRI - Mech 3.0 + NIST HFC + Modified NIST CF_3I	101	881

3. VALIDATION OF MECHANISM

The chemical kinetic model responsible for calculating the species reaction rates and the total heat release was validated against experimental data. In this section, comparison of the predicted burning velocity with measurements is used to validate the mechanism's capability for modelling the total heat release in the flame zone. Comparison of the detailed flame structure with measurements can verify the mechanism's capability to model individual species reaction rates.

3.1 Burning velocity

Burning velocity is employed by many researchers as the flame suppressing index. In order to highlight the need to update the original NIST $CBrF_3$ inhibition mechanism, the computed burning velocity using the original NIST mechanism was compared with the experimental measurements from Linteris et al. [9], Sanogo et al. [10], Parks and Fletcher [11], and Halpern [12] as shown in Figure 1. It can be observed that the NIST mechanism predicts the burning velocity where the fraction of $CBrF_3$ is less than 0.5% reasonably well, but over-predicts for $CBrF_3$ concentrations higher than 0.5%. Using the modified mechanism, for $CBrF_3$ higher than 0.5%, the prediction matches experimental data with a reasonable error difference. Figure 2 compares the predicted burning velocity for the stoichiometric methane-air system suppressed by varying concentration of CF_3I with the measurements from Noto et al. [3] and Sanogo et al. [10], highlighting the capacity of the modified CF_3I inhibition mechanism to predict the burning velocity with reliable accuracy for CF_3I concentrations up to 2%.

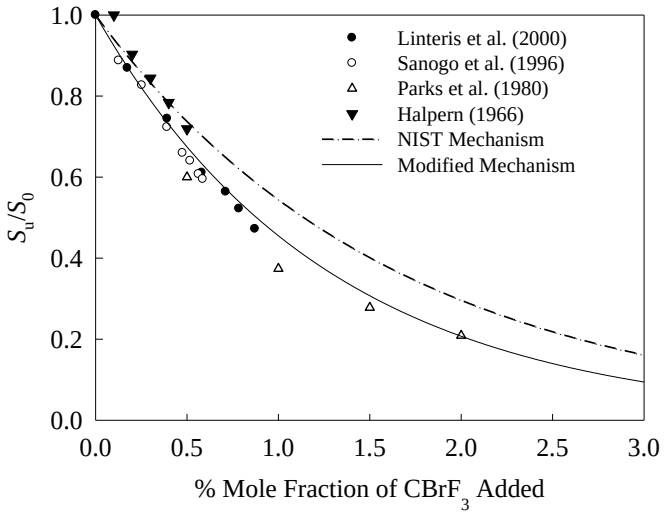

Figure 1 Comparison of experimental and computational burning velocity as a function of concentration of $CBrF_3$ added to atmospheric, stoichiometric CH_4/air premixed flames.

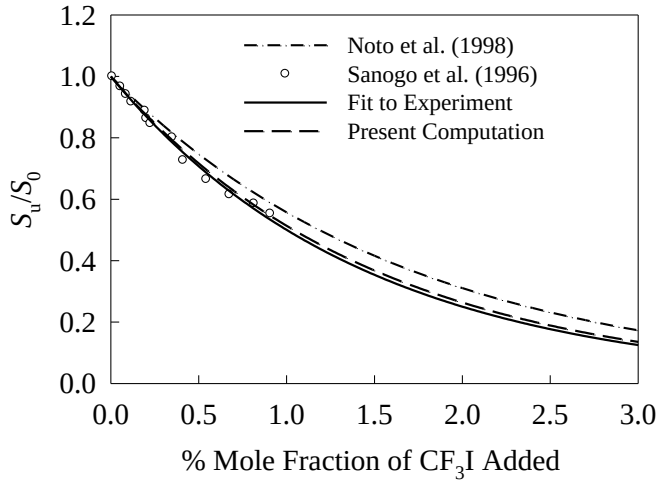

Figure 2 The effect of CF_3I on the normalised burning velocity of the premixed stoichiometric methane-air flames.

3.2 Flame structure of $CH_4/O_2/Ar/CBrF_3$ flames – low pressure

In this section, an assessment of the performance of the updated mechanism to predict flame structure is presented by comparing computational simulations against the measurements by Biordi et al. [13]. These researchers employed a porous plug burner having a diameter of 10 cm and enclosed in a low-pressure housing (0.042 atm) to measure the stable and unstable species profiles in flames using molecular beam sampling and mass spectrometric detection. In the computation using PREMIX model of CHEMKIN, the major parameters are as follows;

- Composition: $CH_4/O_2/Ar/CBrF_3$ = 10.1% : 21.2% : 67.6% : 1.1% ;
- Pressure: P = 0.042 atm;
- Converging criterion: absolute tolerance value = 10^{-12}; relative value = 10^{-6};
- Computational domain: [-2, 2] cm;
- GRAD = 0.15 and CURV = 0.3;
- Burner-stabilized flames + temperature taken from experiments.

The temperature was fitted by the 5-parameter-weibull function:

$$x < x_0 - b(\ln 2)^{\frac{1}{c}} \qquad f(x) = y_0 \tag{1}$$

$$x \geq x_0 - b(\ln 2)^{\frac{1}{c}} \qquad f(x) = y_0 + a\left[1 - e^{-\left[\frac{x - x_0 + b(\ln 2)^{\frac{1}{c}}}{b}\right]^c}\right] \tag{2}$$

where x_0, y_0, a, b, c are the five parameters as determined by least-squares fitting. For the temperature profile in Biordi et al. [13], x_0 = 0.3456, y_0 = 298.9, a = 1568, b = 0.3631, c = 1.748. The fitted curve is shown in Fig. 4-6.

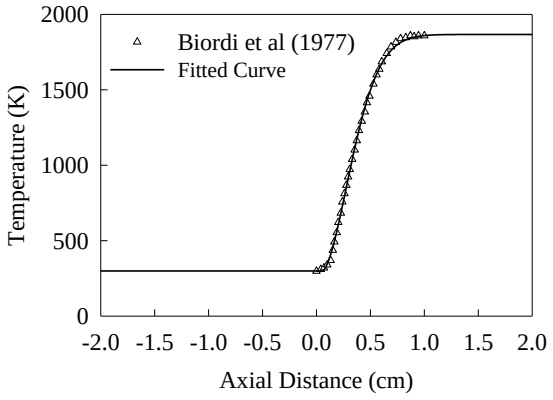

Figure 3 Fitted 5-parameter-Weibull curve to the measuring temperature of Biordi et al. [13].

As shown in Figure 4, the modified mechanism shows improved performance in predicting intermediate profiles compared with the original NIST mechanism. Figure 5 highlights the improvement of the CH_3 profile using the modified mechanism over the original NIST mechanism. Likewise in Figure 6, the HBr profile predicted by the modified mechanism closely matches experimental data. The original NIST mechanism tended to over-predict CH_3Br and under-predict HBr concentrations.

The major reactants profiles predicted by the original and modified $CBrF_3$ are essentially unchanged. Figures 7-9 present the major species profiles of CH_4, O_2 and

$CBrF_3$ respectively, highlighting that showing no significant differences exist between the original and modified $CBrF_3$ inhibition mechanisms for these species.

Above all, both the original and modified mechanism predict quite satisfactory the flame structures for burner-stabilized methane/O_2/Ar/$CBrF_3$ premixed flames at low pressure P = 0.042 atm. The modified mechanism, aimed at improving the CH_3Br concentration profile, does not diminish the good capability of the mechanism to predict burning velocities and the profiles of major species, and improves the profiles of intermediate species compared to the original NIST mechanism.

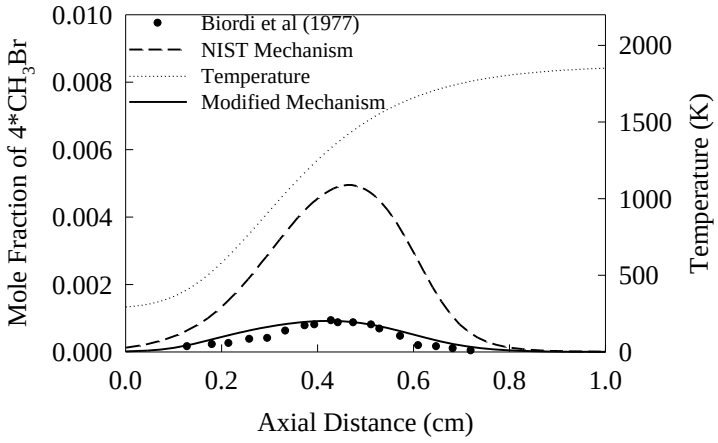

Figure 4 Mole fraction profile comparison of 4×CH_3Br calculated with NIST mechanism and modified.

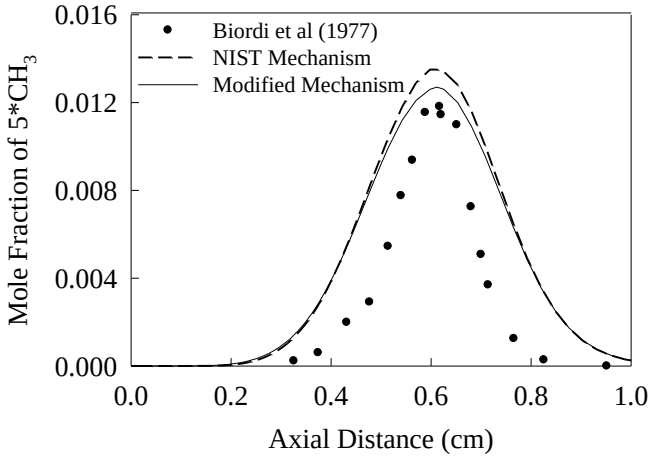

Figure 5 Mole fraction profile comparison of 5×CH_3 calculated with NIST mechanism and modified.

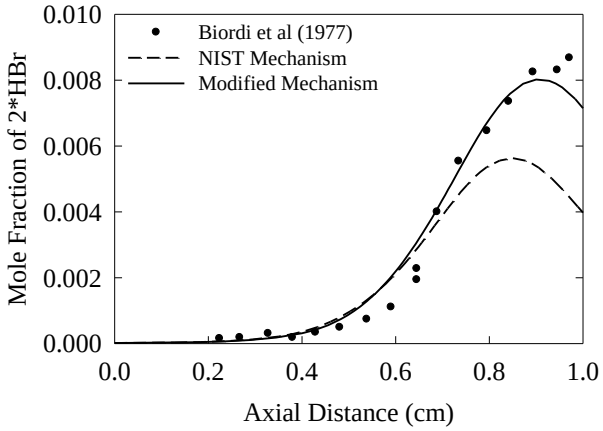

Figure 6 Mole fraction profile comparison of 2×HBr calculated with NIST mechanism and modified.

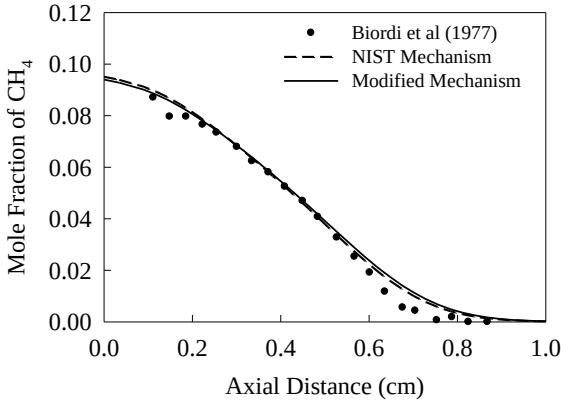

Figure 7 Mole fraction profile comparison of CH_4 calculated with NIST mechanism and modified.

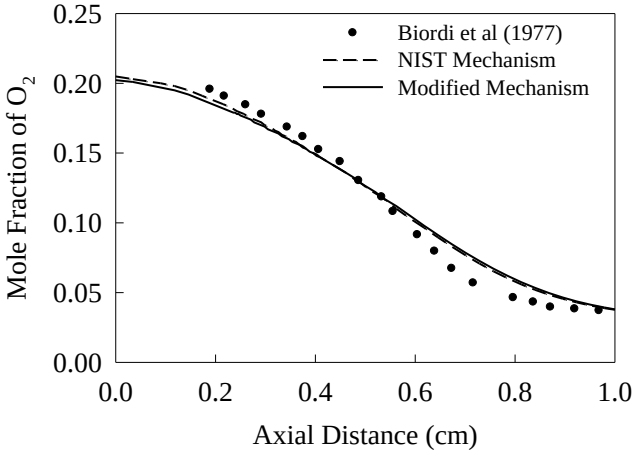

Figure 8 Mole fraction profile comparison of O_2 calculated with NIST mechanism and modified.

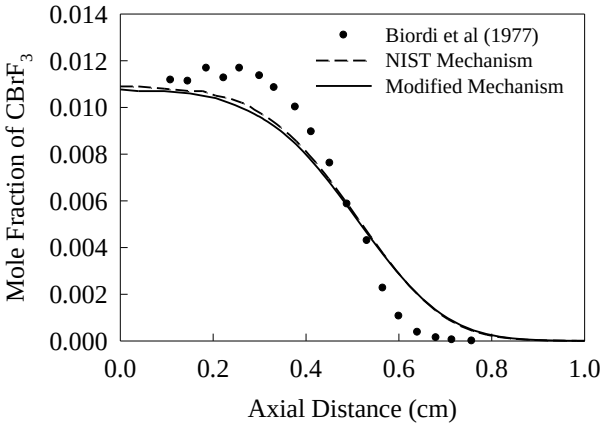

Figure 9 Mole fraction profile comparison of $CBrF_3$ calculated with NIST mechanism and modified.

3.3 Flame structure for $CH_4/O_2/Ar/CF_3I$ flames – atmospheric pressure

The modified mechanism is assessed against the experimental measurements of Sanogo et al. [10], who used molecular beam mass spectrometry to obtain concentration profiles for methane flames stabilised over a water cooled flat burner for $CH_4 : Ar : O_2 : CF_3I = 0.168 : 0.336 : 0.486 : 0.005$.

The Premix model does not consider heat losses due to radiation, or the heat transfer between gas phase and burner surfaces, and as such for the flame structure calculations, the energy balance equation is replaced by the experimentally obtained temperature profiles and these data are used in the computational simulation. The temperature profiles for calculating flame structures are extracted from experiments by Sanogo et al. [10]. According to Sanogo et al. [10], the measured temperature depends on the distance d_{ts} between the thermocouple and the sampling cone, and the temperature profiles for d_{ts} of 0.2 and 20 cm (corresponding to low and high temperature profiles) are presented in Fig. 5.2 of Sanogo et al. [10]. The measured temperature profiles are fitted by the following function

$$T = T_0 + \frac{a}{1 + e^{-\frac{x - x_0}{b}}} + cx \qquad (3)$$

and the corresponding values for the coefficients are given in Table 2. Based on the fitted low and high temperature profiles, a corrected temperature is constructed as follows,

$$T = T_{\text{Low}} \text{ for } x < 0.3 \qquad (4)$$

$$T = T_{\text{Low}}\left[1 - \frac{0.35(x - 0.3)}{0.3}\right] + T_{\text{High}}\frac{0.35(x - 0.3)}{0.3} \text{ for } x \geq 0.3 \qquad (5)$$

in which T_{low} and T_{high} are the low and high temperatures at location x calculated by the fitted functions as defined in Table 2.

The corrected temperature is utilised as the temperature input to the PREMIX computations. It can be seen from Figures 11 and 12 that the modified mechanism can predict the concentration profiles for CF_3I and CO reasonably well. This is also true for H and I radicals for distances less than 0.8 and 0.4 cm, respectively according to figures 13 and 14. It is suggested that the difference between the measurements and prediction of other species is due to (1) inaccuracy in thermo-kinetic parameters; (2) problems with sampling intermediate species; and (3) accuracy of temperature measurements of the thermocouples. However, overall, the modified mechanism provides reasonable predictions of the structure of low pressure methane-O_2-Ar-CF_3I premixed flames.

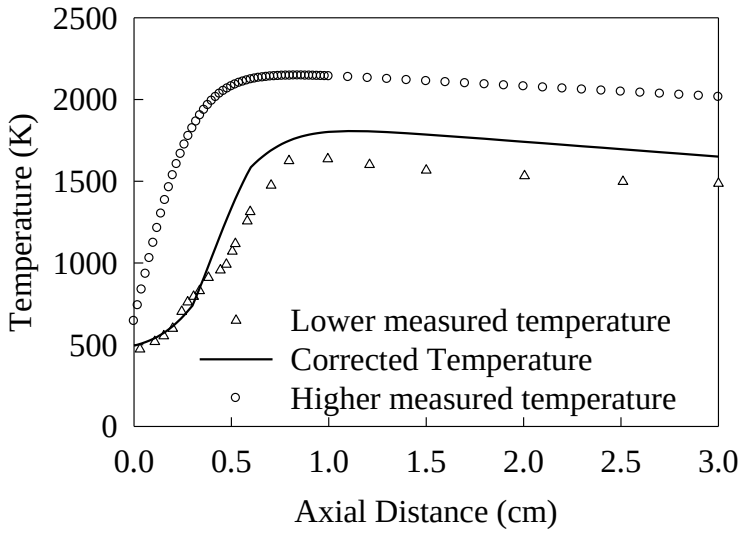

Figure 10 Corrected temperature profile, based on experiments from Sanogo et al. [10], used as input for premixed flame structure calculations.

Table 2. Fit coefficients for low and high measured temperature profiles from Sanogo et al. [10] in the form of Eq. 3.

	a	b	c	x_0	T_0
Low	1341.7	0.1586	-105.07	0.4696	427.83
High	2714.4	0.1386	-64.31	0.0425	506.07

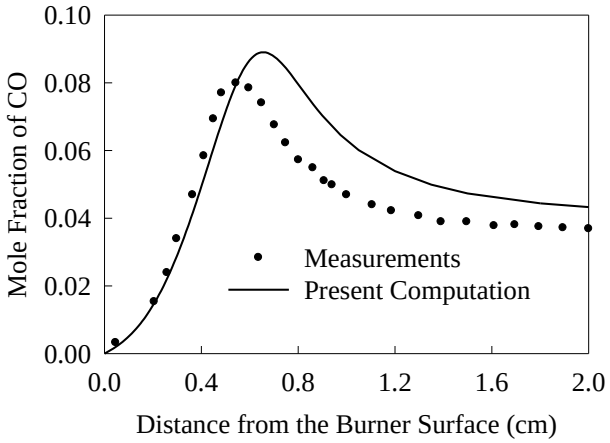

Figure 11 Comparison of CO measured in experiments and predictions from the modified mechanisms: • - experiments of Sanogo et al. (1996); solid line – simulation.

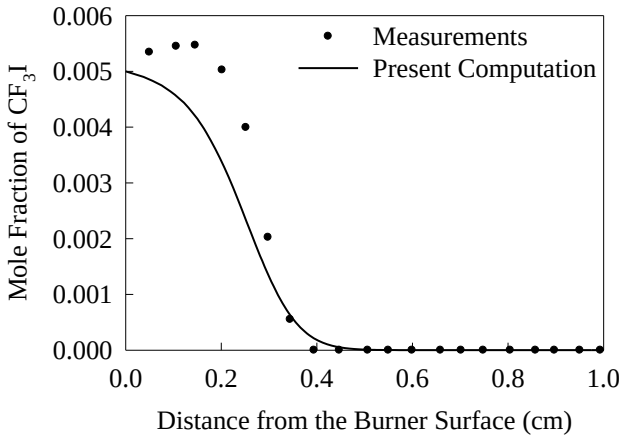

Figure 12 Comparison of CF_3I measured in experiments and predictions from the modified mechanisms: • - experiments of Sanogo et al. (1996); solid line – simulation.

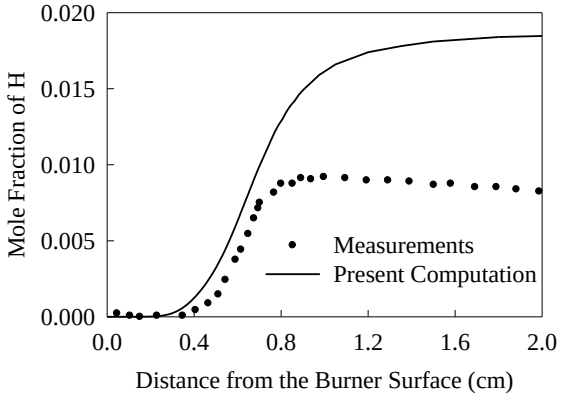

Figure 13 Comparison of H measured in experiments and predictions from the modified mechanisms: • - experiments of Sanogo et al. (1996); solid line – simulation.

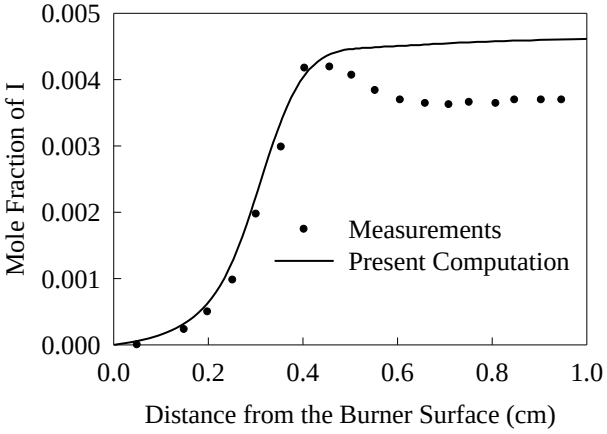

Figure 14 Comparison of I measured in experiments and predictions from the modified mechanisms: • - experiments of Sanogo et al. (1996); solid line – simulation.

4 RESULTS AND DISCUSSION

4.1 Effectiveness of Br_2 and HBr compared with I_2 and HI in methane and methanol fuelled premixed flames

Additional details for the present computations are described by Luo et al. [4]. Stoichiometric methane/methanol air flames suppressed by varying concentrations of Br_2, I_2, HBr and HI were studied numerically by the modifying the source codes of CHEMKIN II. Table 3 summarises the key properties of methane/methanol – air premixed flames from the modified PREMIX software. Included in table 3, the inhibition index was derived by fitting the burning velocity as a function of inhibitor concentration in terms of $\frac{S_{ui}}{S_0} = e^{-bx_i}$ in which S_u and S_0 are the burning velocities with and without inhibitor and x_i is the mole fraction of the inhibitor. The flame temperature and the burning velocities were obtained for stoichiometric methane/methanol – air premixed flames suppressed by 2% of Br_2, I_2, HBr and HI.

It can be observed from Table 3 that the flame temperature is almost independent of the burning velocity, suggesting that the flame temperature should not be used as the flame suppressing index. It should be pointed out that the higher the inhibition index b, the higher the suppressing effectiveness for the inhibitor. As shown in Figure 15(a), Br_2 in the methane-air premixed flame has the highest suppressing effectiveness among all flame systems, and in the methanol-air premixed flame I_2 has higher suppressing effectiveness than Br_2. In the methane-air premixed flames, the suppressing effectiveness of HBr is higher than that of HI as shown in Figure 15(b). However, in the methanol-air premixed flames, HI has a slightly higher suppressing effectiveness than HBr. These observations are consistent with the

methane/methanol-air premixed flames suppressed by CF_3I and $CBrF_3$ as reported in Luo et al. [4].

Table 3 Properties of CH_3OH, CH_4 – air premixed systems with and without inhibitors.

Items	**CH_3OH-air**		**CH_4-air**	
Burning velocity (cm/s)	47.13		39.76	
Flame temperature (K)	2239		2230	
Items	**CH_3OH-air-Br_2**	**CH_3OH-air-I_2**	**CH_4-air-Br_2**	**CH_4-air-I_2**
Inhibition index (*b*)	60.68	81.79	124.18	94.93
Flame Temperature (K)	2156	2123	2135	2135
Burning velocity (cm/s)	15.89	9.64	5.50	5.51
Items	**CH_3OH-air-HBr**	**CH_3OH-air-HI**	**CH_4-air-HBr**	**CH_4-air-HI**
Inhibition index (*b*)	29.25	30.27	64.71	42.87
Flame Temperature (K)	2198	2187	2182	2196
Burning velocity (cm/s)	26.26	23.28	10.27	16.23

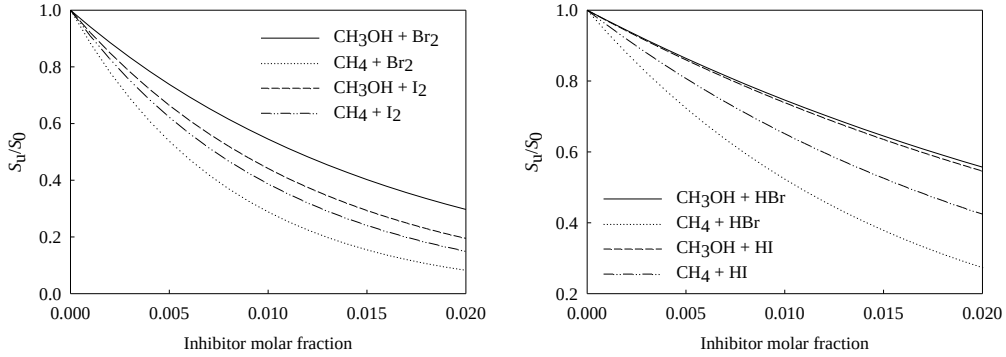

(a) (b)

Figure 15 Variation of the normalized burning velocity vesus inhibitor molar fraction for methane/methanol air flames suppressed by Br_2, I_2, HBr and HI.

4.2 **Reaction Pathway and Inhibition Cycle**

In order to develop an explanation for the difference in effectiveness of Br_2 and HBr over I_2 and HI in the methane and methanol fuelled premixed flames, reaction pathway analysis, based on the bromine/iodine atom flux, is developed and discussed. Integrating the bromine/iodine atom flux to quantify the inhibition reaction pathways has two major advantages over the more traditional carbon atom flux analysis: (1) The key bromine/iodine-containing species that do not contain carbon such as HBr (HI), Br (I), BrO (IO), BrOH (IOH) and Br_2 (I_2) are included in the reaction pathway; (2)

By reducing the number of target species in the inhibition pathway makes, the importance of specific reactions is made clearer.

Figures 16-23 present reaction pathways for stoichiometric methane/methanol-air flames seeded with 2.0% of Br_2, I_2, HBr and HI, with the arrows connecting the species of special interest. The thickness of the connecting arrow is proportional to the corresponding bromine/iodine atom flux transferred. It can be observed from Figures 16-19 that HBr → Br and Br → HBr are important bromine atom transfering reactions both in methane-methanol air premixed flames suppressed by Br_2 and HBr. From these figures, there exists the following major inhibition cycles:

HBr → Br → HBr cycle:

$HBr + H = Br + H_2$ (R1)

$HBr + OH = Br + H_2O$ (R2)

$Br + HCO = HBr + CO$ (R3)

$CH_2O + Br = HCO + HBr$ (R4)

$CH_3OH + Br = CH_2OH + HBr$ (for methanol fuelled flames) (R5)

$CH_4 + Br = CH_3 + Br$ (R6)

HBr → Br → Br_2 → HBr cycle:

$HBr + H = Br + H_2$ (R1)

$HBr + OH = Br + H_2O$ (R2)

$2Br + M = Br_2 + M$ (R6)

$BrOH + Br = Br_2 + OH$ (R7)

$Br_2 + H = Br + HBr$ (R8)

$Br \rightarrow Br_2 \rightarrow Br$ cycle:

$$2Br + M = Br_2 + M \quad \text{(R6)}$$

$$BrOH + Br = Br_2 + OH \quad \text{(R7)}$$

$$Br_2 + H = Br + HBr \quad \text{(R8)}$$

The major difference between the methane and methanol fuelled flames is the decomposition reaction of CH_3OH to CH_2OH via Br atom (reaction R5). Comparing Figures 16-17 for HBr suppressed methane/methanol air premixed flames, the conversion of Br to HBr becomes more significant for a methanol-air premixed flame due to the higher rate of reaction of CH_3OH. In contrast, comparing Figures 20-21 for HI suppressed methane/methanol air premixed flames, CH_3OH plays little role in conversion from I to HI or HI to I, and the inhibition cycle $I_2 \rightarrow I \rightarrow I_2$ become more significant for CH_3OH-air-HI system with respect to the CH_4-air-HI flame system.

As shown in Figures 18-19 and Figures 21-22 for methane/methanol-air premixed flames suppressed by Br_2 or I_2, inhibition cycles $I_2 \rightarrow I \rightarrow I_2$ or $Br_2 \rightarrow Br \rightarrow Br_2$ become more important with respect to $HI \rightarrow I \rightarrow HI$ or $HBr \rightarrow Br \rightarrow Br_2$, and especially for the CH_3OH-air-I_2 premixed flame $I_2 \rightarrow I \rightarrow I_2$ becomes much more significant than $HI \rightarrow I \rightarrow HI$. Certainly, CH_3OH also contributes significantly(50.85%) to the conversion from Br to HBr in the methanol-air-I_2 system, and as shown in Figure 22 there is close to zero contribution from CH_3OH for conversion from I to HI.

Based on these analyses, the major reason for the higher suppressing effectiveness of Br_2 and HBr over I_2 and HI in the methane/methanol sir premixed flames is the enhanced contribution of the Br atom in the fuel decomposition. In addition, the

enhancement of the inhibition cycles $I_2 \rightarrow I \rightarrow I_2$ with respect to $HI \rightarrow I \rightarrow HI$ in the methanol-fuelled premixed flames are likely to be responsible for this phenomenon.

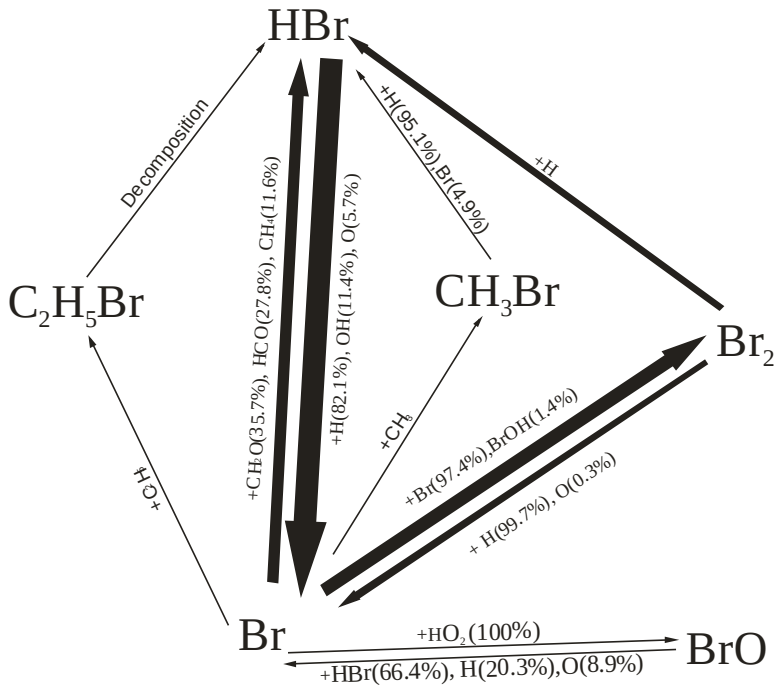

Figure 16 Reaction pathways for stochiometric CH_4 - air flame suppressed by 2.0% HBr.

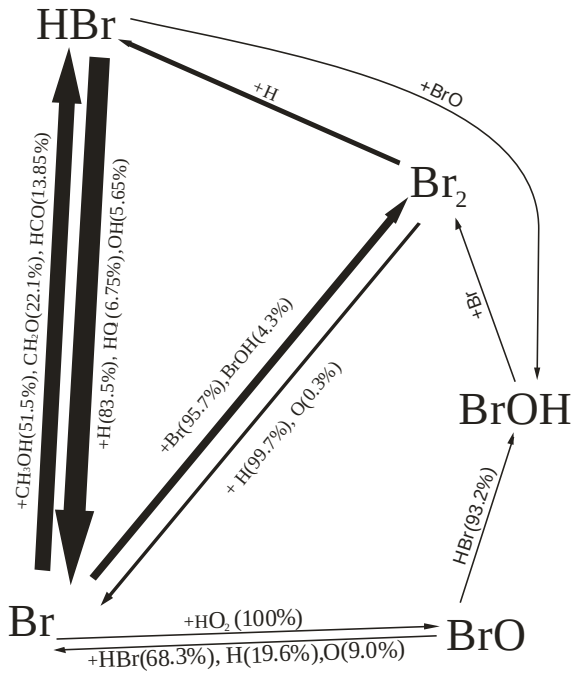

Figure 17 Reaction pathways for stochiometric CH_3OH - air flame suppressed by 2.0% HBr.

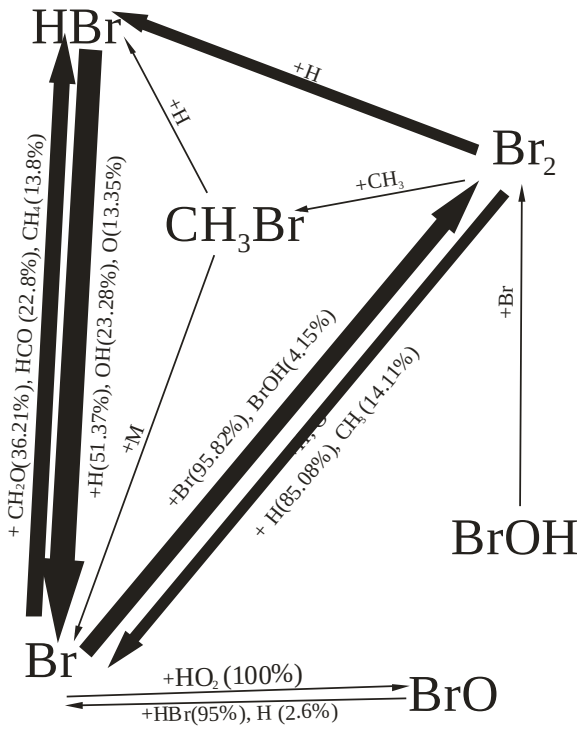

Figure 18 Reaction pathways for stochiometric CH_4 - air flame suppressed by 2.0% Br_2.

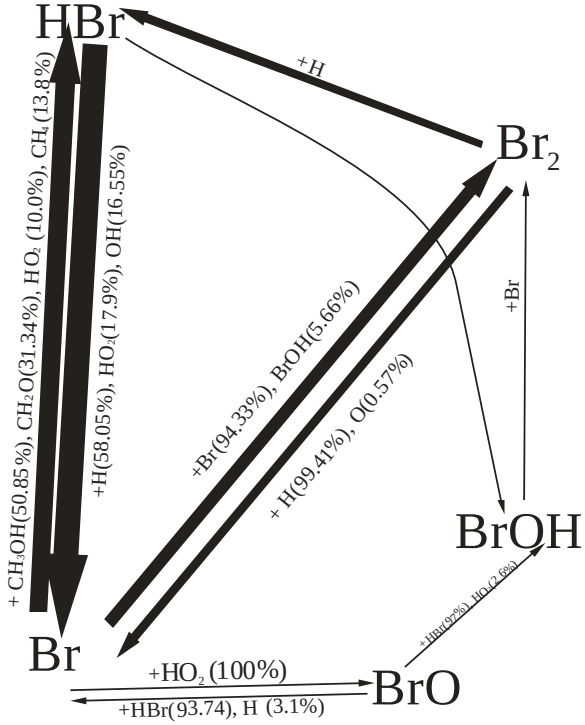

Figure 19 Reaction pathways for stochiometric CH_3OH - air flame suppressed by 2.0% Br_2.

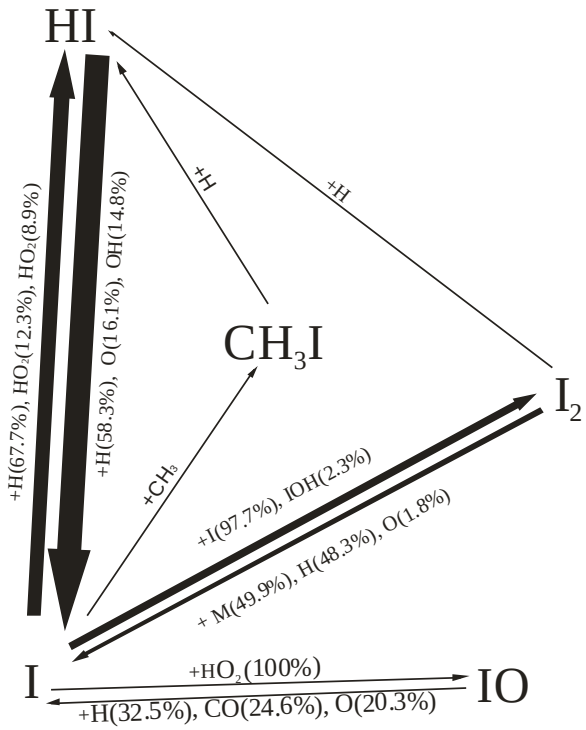

Figure 20 Reaction pathways for stochiometric CH_4 - air flame suppressed by 2.0% HI.

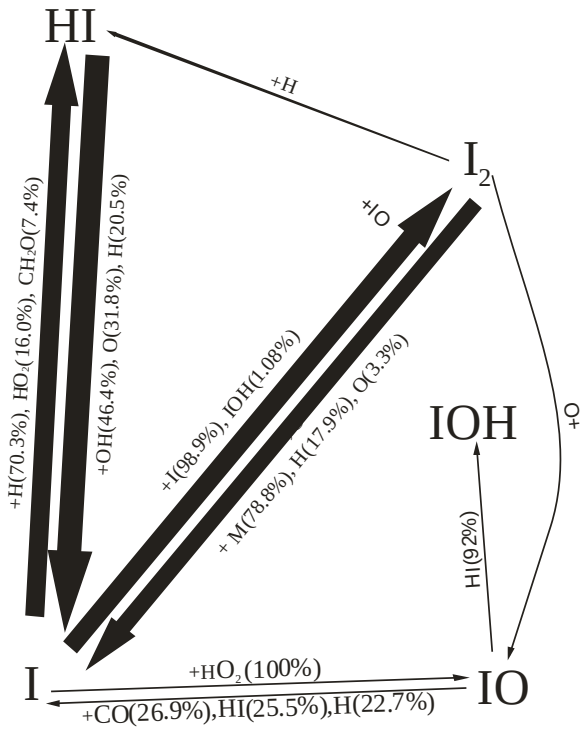

Figure 21 Reaction pathways for stochiometric CH_3OH - air flame suppressed by 2.0% HI.

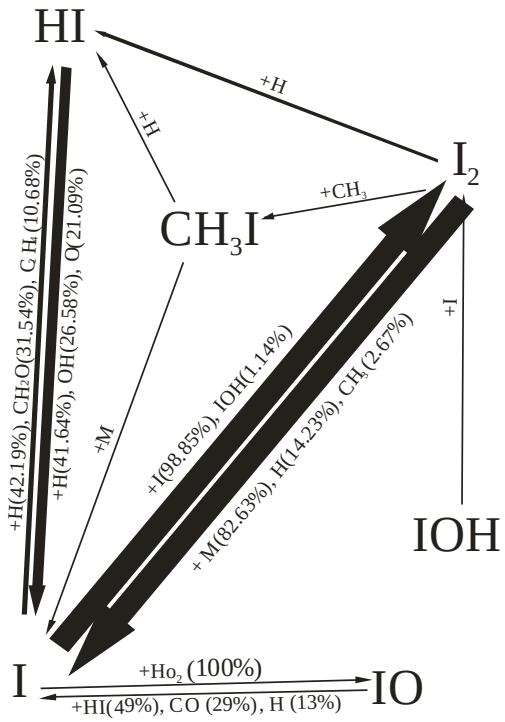

Figure 22 Reaction pathways for stochiometric CH_4 - air flame suppressed by 2.0% I_2.

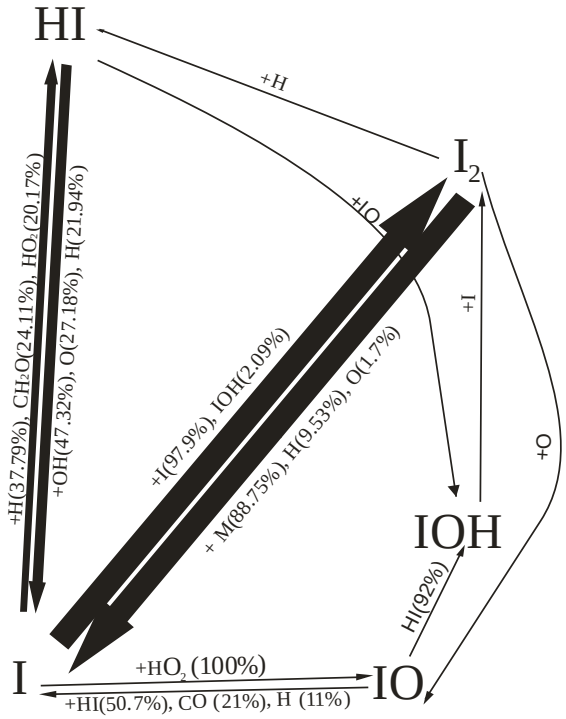

Figure 23 Reaction pathways for stochiometric CH_3OH - air flame suppressed by 2.0% I_2.

5 CONCLUSIONS

Updated CF_3I and $CBrF_3$ inhibition mechanisms were developed and validated against burning velocity data from published sources and flame structure obtained by molecular beam mass spectrometry experiments. Integrated bromine/iodine atomic flux analysis was incorporated into PREMIX II of the CHEMKIN suite of programs to undertake reaction pathway analysis for the new mechanism, having 100 species and 880 reaction steps. Premixed methane/methanol-air flames inhibited by Br_2, HBr, I_2, and HI were analysed. Based on reaction pathway analysis, the effectiveness of Br_2 and HBr over I_2 and HI in the methane/methanol sir premixed flames include:

1. The promoting contribution of the Br atom for fuel decomposition.
2. Enhancement of the inhibition cycles $I_2 \rightarrow I \rightarrow I_2$ with respect to $HI \rightarrow I \rightarrow HI$ in methanol-fuelled premixed flames.

REFERENCES

1. Moore, T.A., C.A. Weitz, and R.E. Tapscott. Update on NMERI Cup-Burner Test Tesults. in *Halon Options Technical Working Conference (HOTWC 1996)*. 1996. Albuquerque, NM.
2. Noto, T., V. Babushok, D.R. Burgess, Jr., A. Hamins, and W. Tsang, Effect of halogenated flame inhibitors on C1-C2 organic flames. Symposium (International) on Combustion, [Proceedings], 1996. **26th**(Vol. 1): p. 1377-1383.
3. Noto, T., V. Babushok, A. Hamins, and W. Tsang, Inhibition Effectiveness of Halogenated Compounds. Combustion and Flame, 1998. **112**(1-2): p. 147-160.

4. Luo, C., B. Dlugogorski, and E. Kennedy, Influence of CF_3I and $CBrF_3$ on Methanol–Air and Methane–Air Premixed Flames. Fire Technology, 2008. **44**(3): p. 221-237.

5. Smith, G.P., D.M. Golden, M. Frenklach, N.W. Moriarty , B. Eiteneer, M. Goldenberg, C. Bowman, R.K. Hanson , S. Song, C.C. Gardiner, V.V. Lissianski, and Z. Qin. Gri-MECH 3.0. 2003 [cited; Available from: http://www.me.berkeley.edu/gri_mech/.

6. Burgess, D.R., Jr., M.R. Zachariah, W. Tsang, and P.R. Westmoreland, Thermochemical and chemical kinetic data for fluorinated hydrocarbons. Progress in Energy and Combustion Science, 1995. **21**(6): p. 453-529.

7. L'Esperance, D., B.A. Williams, and J.W. Fleming, Intermediate species profiles in low pressure premixed flames inhibited by fluoromethanes. Combustion and Flame, 1999. **117**(4): p. 709-731.

8. Linteris, G.T. and G.W. Gmurczyk, Prediction of HF formation during suppression. NIST Special Publication, 1995. **890** (Fire Suppression System Performance of Alternative Agents in Aircraft Engine and Dry Bay Laboratory Simulations, Vol. 2): p. 201-318.

9. Linteris, G.T., M.D. Rumminger, V. Babushok, and W. Tsang, Flame inhibition by ferrocene and blends of inert and catalytic agents. Proceedings of the Combustion Institute, 2000. **28**(Pt. 2): p. 2965-2972.

10. Sanogo, O., J. Delfau, R. Akrich, and C. Vovelle, A comparative study of the structure of CF_3Br and CF_3I doped methane flames. Journal de Chimie Physique et de Physico-Chimie Biologique, 1996. **93**(11-12): p. 1939-1957.

11. Parks, D.J. and E.A. Fletcher, Fluorocarbon combustion studies. V. Trifluorochloromethane- and trifluorobromomethane-fluorine flames. Combustion and Flame, 1969. **13**(5): p. 487-494.

12. Halpern, C., Effect of some halogenated hydrocarbons on the flame speed of CH_4. J. Res. Natl. Bur. Std., A, 1966. **70**(2): p. 133-141.

13. Biordi, J.C., C.P. Lazzara, and J.F. Papp, Flame structure studies of bromotrifluoromethane-inhibited methane flames. 3. The effect of 1% bromotrifluoromethane on composition, rate constants, and net reaction rates. Journal of Physical Chemistry, 1977. **81**(12): p. 1139-45.